

A novel method for realistic DWI data generation

Daniele Perrone¹, Jan Aelterman¹, Ben Jeurissen², Aleksandra Pizurica¹, Wilfried Philips¹, and Jan Sijbers²

¹IPI-TELIN-IMINDS, University of Gent, Gent, East Flanders, Belgium, ²Vision Lab, University of Antwerp, Antwerp, Belgium

Diffusion Weighted Imaging (DWI) was introduced to explore the human connectome in vivo; although many fiber tractography (FT) algorithms exist, proving the effectiveness of their estimates is challenging. We present a biologically and physically realistic software phantom, with brain-like fibres configuration and images, fully tuneable in terms of ‘simulated acquisition’ parameters: a realistic bench test for quantitative analyses of every DWI-related algorithm.

High quality DW data was acquired from a healthy volunteer on a 3T scanner, using an 8-channel receiver head coil. Diffusion weightings of $b = 0$ and 2800 s/mm^2 were applied in 5 and 75 directions, respectively. In addition, 5 $b = 0 \text{ s/mm}^2$ images were acquired with reversed phase encoding, for the purpose of EPI correction. Other imaging parameters were: TR/TE: 9500/100 ms; voxel size: $2 \times 2 \times 2 \text{ mm}^3$; matrix: 120×120 ; slices: 68; NEX: 1. A T1 image was also acquired, to aid identification of the different tissue types.

Post-processing: DW images were corrected for motion and Eddy current distortions using the approach of Raffelt.¹ To ensure a proper match between the T1 data and the DW data, all DW images were corrected for EPI distortions using FSLs ‘topup’.² Four tissue types (cerebrospinal fluid (CSF)/cortical gray matter (CGM)/deep matter (DGM)/white matter (WM)) were segmented on the T1 image following a pipeline proposed by Smith.³ On the corrected data set, ACT³ was performed with iFOD2, resulting in a set of 5×10^7 streamlines with high anatomical plausibility, further reduced down to 5×10^6 streamlines using SIFT,⁴ to improve correspondence with the DW data and account for seeding biases. The four tissue type segmentation maps \mathbf{S} and the final tractogram were used as ground truth input for our phantom generation pipeline. MR images come from a linear combination of the excited-state protons signals, so our model has a linear relationship with \mathbf{S} :⁵ the anatomical part of the signal $S(\mathbf{r}, j)_0$ depending on the tissue j and the voxel \mathbf{r} is calculated based on the IRSE sequence and combined via the coefficients $a(\mathbf{r}, j)$ of \mathbf{S} , and the same holds for the DW signal loss. The proposed attenuation model $S(\mathbf{r}, q)/S(\mathbf{r})_0 = \sum_{j=1}^M a(\mathbf{r}, j) \sum_{i=1}^{N(\mathbf{r})} \frac{1}{N(\mathbf{r})} A(p(j), q, i)$ accounts for diffusion patterns $A(p(j), q, i)$

coming from the $N(\mathbf{r})$ fibres and the M tissues in \mathbf{r} . The models used are the state of the art in terms of accuracy⁶. In this work, the acquisition parameters can be tuned: the MR parameters TE, TR, TI , the DWI q and the tissue intrinsic ones $p(j)$, set according to a method of Panagiotaki,⁶ making the proposed technique flexible. We noticed FA maps in agreement with real data, and that a reduction in the resolution leads to realistic Gibbs effect (fig. 1). We performed FT according to our earlier method⁷ on two phantoms with $b=2500$ and $b=1500 \text{ s/mm}^2$ (respectively red and green, fig. 2): we can extract bundles whose arrangement is very complex and realistic. Small differences in connectomes exist and were expected. Our phantom show a good consistency with the inputs and with anatomical and WM structures observed in real data.

The parameters $p(j)$ could be re estimated from the newly released Human Connectome Project dataset. Further validation on the phantom is needed, to verify that the correct connectivity among ‘simulated brain regions’ is inferred. After introducing noise or artefact in the phantom, any image restoration or FT technique can be quantitatively validated.

Bibliography

1. Raffelt et al. Apparent Fibre Density: A novel measure for the analysis of diffusion-weighted magnetic resonance images. *NeuroImage*. 2012; 59(4):3976-3994
2. Andersson JLR et al. How to correct susceptibility distortions in spin-echo echo-planar images: application to diffusion tensor imaging. *NeuroImage*. 2003; 20(2):870-888.
3. Smith RE et al. Anatomically-constrained tractography: improved diffusion MRI streamlines tractography through effective use of anatomical information. *Neuroimage*. 2012; 62(3):1924-38.
4. Smith RE et al. Spherical-deconvolution informed filtering of tractograms. *Neuroimage*. 2013; 67:298-312.
5. Drobniak I et al. Development of an FMRI Simulator for Modelling Realistic Rigid-Body Motion Artifacts. *MRM*. 2006; 56(2):364-380.
6. Panagiotaki E et al. Compartment models of the diffusion MR signal in brain white matter: A taxonomy and comparison. *NeuroImage*. 2012; 59(3):2241-2254.
7. Jeurissen B et al. Probabilistic fiber tracking using the residual bootstrap with constrained spherical deconvolution. *Hum Brain Mapp*. 2011; 32(3):461-79.

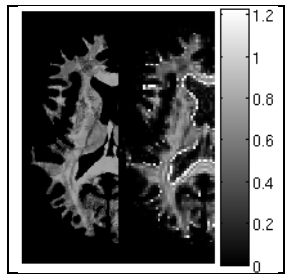


Fig.1: FA image, phantom. Left: $1 \times 1 \times 1 \text{ mm}^3$ resolution. Right: $2 \times 2 \times 2 \text{ mm}^3$ resolution.

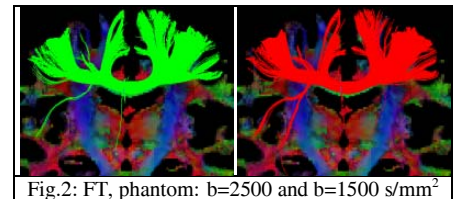


Fig.2: FT, phantom: $b=2500$ and $b=1500 \text{ s/mm}^2$